

Robust Three-Dimensional Model for Dentate Mandible with Temporomandibular Joint Based on Actual Computed Tomography Data

Tamer M. Nassef¹, Nahed H. Solouma², Mona K. Marie³, Mohamed Elkhodary³, Abdullah S. Ahmed^{1,4} and Yasser M. Kadah⁴

¹Computer Engineering Department, Misr University for Science & Technology, 6th of October, Egypt, (proff.tamer@hotmail.com)

²Laser in Engineering, NILES, Cairo University

³Tissue Engineering center, Faculty of Dentistry, Alexandria University

⁴Systems & Biomedical Engineering Department, Cairo University, Giza, Egypt,

Abstract:

In this paper, numerical methods are used to build a three-dimensional (3D) model for human mandible with multi-objects from two-dimensional (2D) images captured by computed tomography (CT) scanner device. Three steps are used to evaluate realistic model; First step, segmentation techniques; are used to eliminate the undesired tissues, Second step, multi-object reconstruction technique; are used to evaluate both mandible bones and teeth, final step, texture models are generated. The output models are validated in comparison with the actual 3D model, which are generated by the CT scanner; they are meshed by tetrahedral elements to prepare the geometry for the finite elements analysis (FEA). Preliminary results are obtained for intensity measurements of teeth are presented.

1. Introduction:

The use of numerical methods such as finite element methods (FEM) has been adopted in solving complicated geometric problems, as it is very difficult to achieve an analytical solution. FEM is a technique for obtaining a solution to complex mechanical problems by dividing the domain problem into a collection of much smaller and simpler domains (elements) where field variables can be interpolated using shape functions [3]. In 1977, Weinstein [1] was the first to use FEM in implant dentistry. Subsequently, FEM was rapidly applied in many aspects of implant dentistry. Atmaram and Mohammed [2]-[4] analyzed the stress distribution in a single tooth implant, to understand the effect of elastic parameters and geometry of the implant, implant length variation, and pseudo-periodontal ligament incorporation. Borchers and Reichart [5] performed a three-dimensional (3D) FEM of an implant at different stages of bone interface development. Cook, et al. [6] applied it in porous rooted dental implants. Meroueh, et al. [7] used it for an osseointegrated cylindrical implant. Williams, et al. [8] carried it out on cantilevered prostheses on dental implants. Akpınar, et al. [9] simulated the combination of a natural tooth with an implant using FEM.

Image scanners devices such as computed tomography (CT), magnetic resonance imaging (MRI) or positron emission tomography (PET) are nowadays a standard instrument for diagnosis. Among these devices, CT images are often preferred by diagnosticians since they have high Signal-to-Noise ratio and good spatial resolutions, thus providing accurate anatomical information about the visualized structures principally for bones. These good image qualities and the advances in the digital image processing techniques; motivate the great deal of research work aimed at the development of computerized methods for analyzing human mandible and to generate 3D volume renders [10]. Construction of 3D models from two-dimensional (2D) images has a potential in dentistry studies. Ruijven et al [11] analyzed the effect of an inhomogeneous distribution of mineralization on the stress and strain distributions in the human mandibular condyle during static clenching by building FEM model with a voxel conversion technique. G. Tognola et al [12]-[14] created a realistic 3D model of patient mandible from CT images to help in the pre-surgical phase, and used gradient vector flow snake parameters in order to achieve more accurate contours segmentation of nerve mandibular scans.

G. Pileicikiene et al [15] performed a 3D model of human mandible from images for a dead person. Ming Chen et al [16] chose the same condition with commercial software to achieve comparison between dead and alive 3D models. Zhan Liu et al [17] used commercial software to generate a 3D model for a human mandible including the Temporomandibular Joint (TMJ) and verified the different types of mandible bones (cortical and trabecular). Reina et al [18] presented a 3D surface model of mandible based on morphological analysis with standard distances without case study. The main objective of the present study is to generate 3D models for the human mandible with TMJ based on actual CT data with multi-objects segmentation. New reconstruction techniques are used to create 2½D and 3D models, textured by actual CT raw images. Three phases will be evaluating the 3D models defined as follows; Segmentation phase based on CT data, Multi-object reconstruction phase and texture phase.

2. Material and methods:

The dentate mandible was scanned with SIEMENS/Esprit 130 KV – 90.0000 mAs CT machine. The pixel size of the scanner is 512x512 pixels, and 0.391x0.391 mm is equal to the distance between CT slice planes. Totally 71 images were obtained (Figure 1), raw data was in Digital Imaging and Communications in Medicine (DICOM) format, with 4096 gray levels in the range [-1024, +3071], directly related to the Hounsfield units (HU).

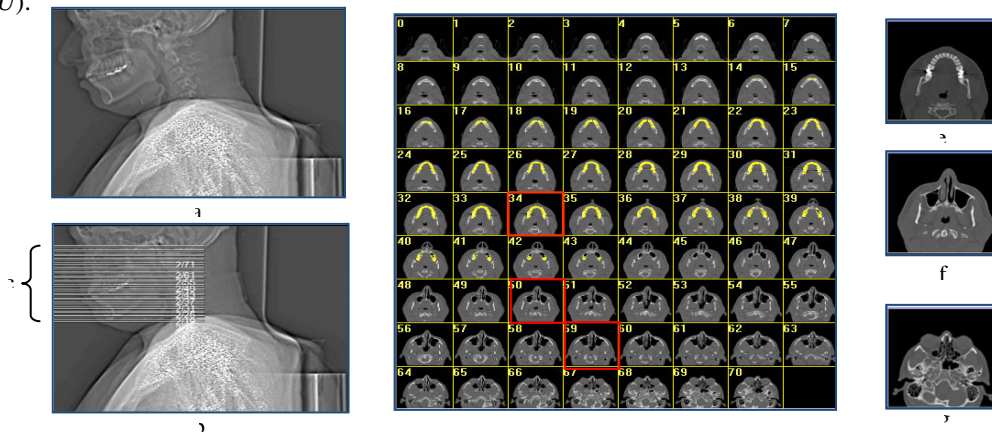


Figure 1. Data acquisition from CT, (a) and (b) patient alignment x-ray, (c) mandible regions position, (d) all slices axial planes, red rectangles displays (e), (f), and (g) sample slices positions.

The human mandible anatomy consists of three different parts; first part defines the mandible body and teeth positions, that appears at CT slices from (0 - 43), second part defines the two lateral sides of mandible, which called as "Ramus", that become visible at slices (44-54) and the third part defines the TMJ region with "coronoid process", this can be explained with free hand draws of mandible confirmed by AutoCAD program figure 2. [19].

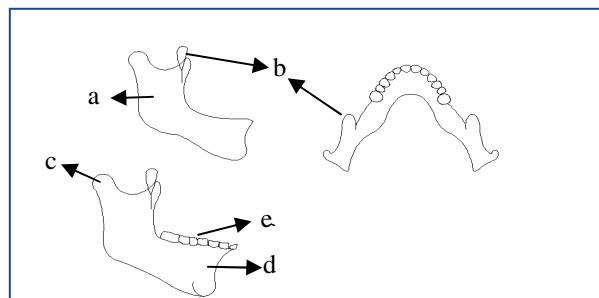


Figure 2. The human mandible anatomy, (a) Ramus region, (b) coronoid process region, (c) TMJ region (d) mandible body and (e) teeth.

2.1 DICOM information:

DICOM format files carrying all information about CT scanned, table 1, present some of useful information. P. Campadelli et al [20] segmented different tissues based on *HU* range by verified windows defining the tissues pixel positions, each slice has different *HU* range and this helps in applying the threshold technique to eliminate the undesired tissues and focus on the mandible regions only.

Table 1. Information samples carried by DICOM files

Rows	512	Columns	512
Rescale Intercept	-1024	Rescale Slope	1
KVP	130	Reconstruction Diameter	200
Exposure Time	2000	X-ray Tube Current	45

Noise produced by the reflection rays on filling materials affects the *HU* range and the 3D reconstruction of the mandible. These noises can not appear clearly in axial planes, but it evidently become visible at the 3D model as shown in figure 3. G. Tognola et al [14] proposed a segmentation technique to reduce the noises caused by “star-shaped” artifacts, due to dental or mandible metallic implants, this technique based on the threshold method, while P. Campadelli et al [21] used other technique based on selecting the *HU* values, HU_{min} and HU_{max} .

The 3D model and panoramic image are captured from the CT scanner directly without any enhanced or segmented procedures, by the combination between both techniques at [14] and [21] a new technique is produced to reduce all noises from the DICOM raw data without any conversions of formats to keep DICOM information, that used in separating all the mandible regions to build a robust 3D model. The procedures to generate a 3D model are explained in figure 4.

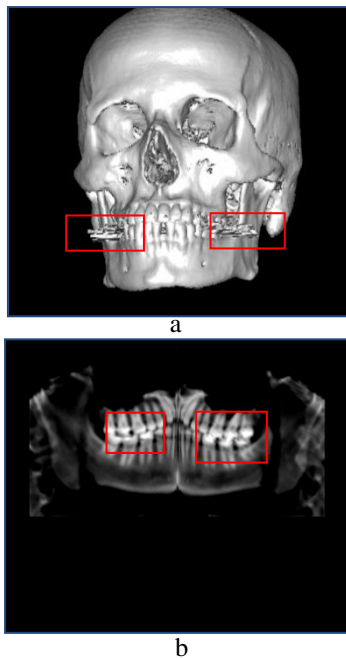


Figure 3. (a) 3D model for a mandible as a part of a skull, (b) panoramic x-ray, the red rectangles refer to the filling cavity materials that cause noises.

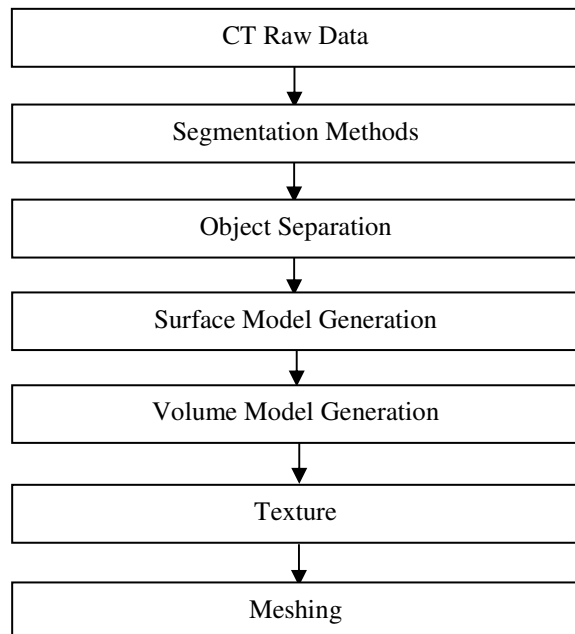


Figure 4. Procedures for generating three-dimensional models and meshing.

2.2- Multi-object reconstruction:

The mandible regions can be separated to multi-objects (i.e. teeth, TMJ, body ...etc); this must be performed during the segmentation phase to evaluate the objects and verify it before generating the 3D model and it is called 2½D models; it is not a complete 3D or 2D as shown in figure 9. This study generates multi-objects of head and neck based on actual CT information extracted from DICOM files, all these objects are described later in section 3. The multi-object reconstruction helps in finite element analysis (FEA); that the FE models will have specific information about organs; this helps in reducing the time of solving the mechanical problems. TMJ and "coronoid process" regions separation processes were difficult since their positions at the back of the face bone as in figure 3. (a). Consequently, proposed segmentation technique is used to extract these regions from the CT slices based on region growing technique, which is implemented with Matlab program. Triangulation process method is used to generate the 2½D models and the marching cubes for the final 3D mode; this is applied for all regions (objects).

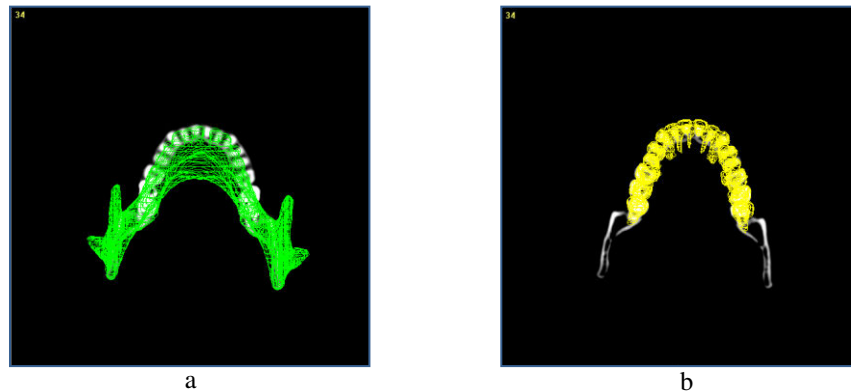


Figure 5. The 2½D reconstruction; (a) mandible with TMJ, (b) mandible teeth.

2.3- Texture 3D model:

After the multi-object reconstruction process; the objects must be enveloped by texture material as shows in figure .6. This material has properties must be defined within the FE program. Section 3 shows other samples of texture materials for different objects (i.e. teeth, skin, skull ...etc).

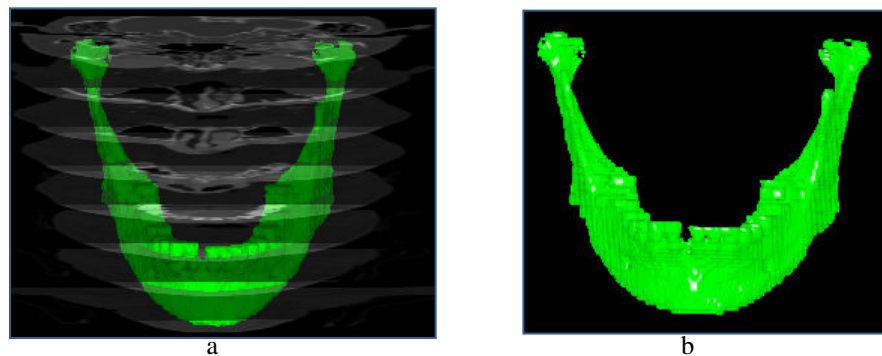


Figure 6. The texture material, (a) CT planes with mandible, (b) mandible textured with bone material.

3. Results:

A computer program was written in Matlab code for implementing the segmentation process applied on all DICOM planes, all planes are assembled with commercial software based on 'OpenGL algorithms'. Multi-objects regions enveloped with texture material to verify their prosperities, figure 7, the teeth textured model at

started from plane (13 – 43), by evaluating the vertex (x,y,z) of model from origin (0,0,0) pixels positions can be calculated. Intensity can be measured by calculating the pixels values multiplied by pixels numbers (1). Preliminary intensity measurements are shows in table 2.

$$Intensity(x) = \sum_{i=1}^n (P_n * P_v) \quad (1)$$

where P_n equal to pixel position and P_v equal to pixel value and i refer to pixel number.

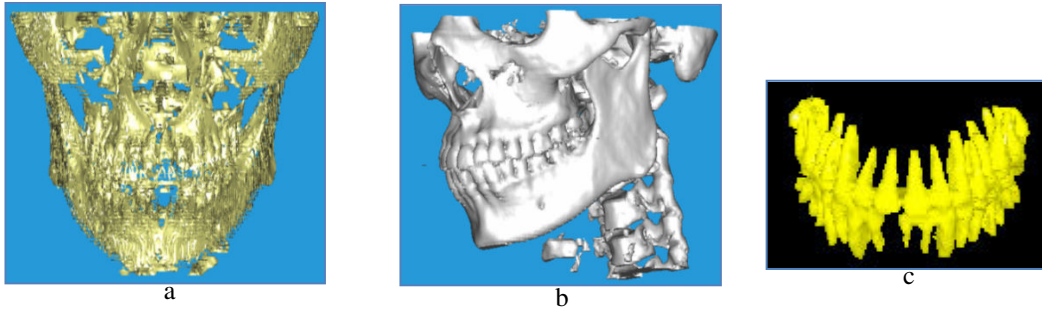


Figure 7. 3D surfaces models, (a) front view for skull without texture enveloping, (b) lateral view textured by bone material, (c) full teeth object extraction.

Table 2. Intensity measurements of teeth

38	2161	265.63,261.24,38.0	6515996	3015.3
39	1945	267.21,266.13,39.0	5835420	3000.2
40	1442	264.42,267.71,40.0	4118520	2856.1
41	1036	271.41,271.51,41.0	2734922	2639.9
42	606	268.14,278.23,42.0	1631745	2692.4
43	272	275.32,268.81,43.0	734706	2715.96
44	72113	264.34,230.99,25.67	218144702	3035.0
16	582	274.29,207.78,16.0	1594598	2739.9
17	873	269.60,205.71,17.0	2386330	2733.5
18	1100	269.02,205.98,18.0	2990182	2718.3
19	1265	268.82,205.25,19.0	3433094	2713.9
20	1541	268.06,206.98,20.0	4220361	2738.7
21	1778	268.09,204.88,21.0	4974909	2798.03
22	2118	269.97,203.97,22.0	6253879	2952.7
23	2320	268.55,207.21,23.0	6962188	3000.94
24	2600	269.67,211.63,24.0	7778765	2991.8
25	3080	269.59,216.60,25.0	9190472	2983.9
26	3579	267.21,216.60,26.0	10960723	3062.5
27	4206	268.81,217.46,27.0	13235639	3146.8
28	4302	264.79,215.06,28.0	13810357	3210.2
29	4829	267.71,223.27,29.0	15337139	3176.04
30	4450	267.05,227.75,30.0	13962937	3137.7
31	4030	264.49,231.13,31.0	12802160	3176.7
32	4108	265.77,238.48,32.0	12629372	3074.3
33	4407	264.80,247.50,33.0	13444604	3050.7
34	4032	261.81,246.58,34.0	12263601	3041.6
35	3445	263.38,249.19,35.0	10509540	3050.7
36	3041	261.39,251.57,36.0	9057583	2978.5
37	2518	263.58,256.95,37.0	7558038	3001.6

The number of pixels are presented in each plane (from 13 to 42) carries the teeth information at column 2, total pixels intensity values are reported at column 3; that it are evaluated by integrated the all intensity values for pixels in each plane. Multi- objects are evaluated based on CT data are shows at figure 8. Those four objects are presented (skin, skull, mandible and tooth), each object is textured by their suitable material with different colors and these textured models can be meshed by tetrahedral elements to prepare it for FEA.

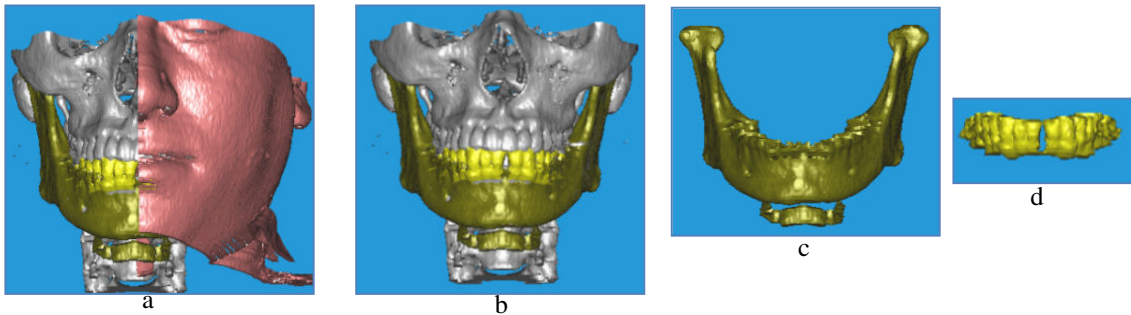


Figure 8. Multi-objects 3D model, (a) all objects with skin section, (b) full skull without skin, (c) full mandible with neck cartilage and without teeth, (d) mandible teeth.

Dental diagnosing are needed more realistic models based on actual CT data; this can be evaluated by using the intensity measures of mandible regions to build a volumetric model as shows in figure 9. The model are textured with actual CT data; that make it displays as x-ray images and teeth roots are appeared, this make the 3D model more realistic.

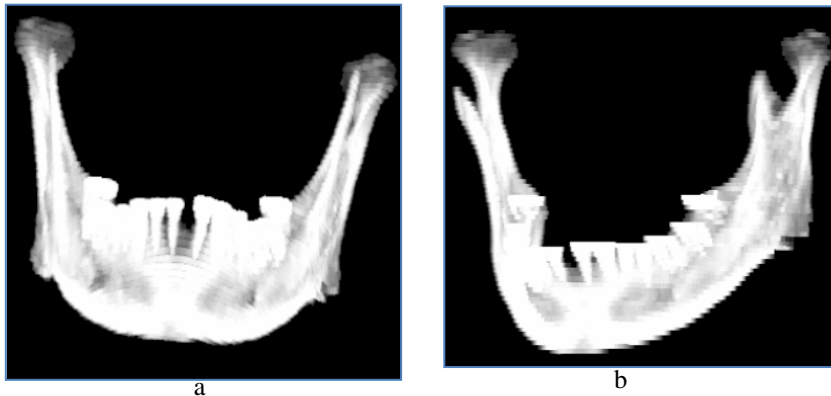


Figure 9. The volume model of full mandible textured with actual plane intensity, (a) front view, (b) angular view to display TMJ and "coronoid process".

4. Conclusion:

Many investigators have evaluated 3D models from CT 2D images. The results of these studies have been approximated for the conversion of images formats, this study provide a realistic 3D model from 2D segmented images scanned with CT scanner device based on actual CT data carried by DICOM files formats. Preliminary results are reported; pixels intensity values and pixels numbers are significant to verify the volumetric 3D model of objects, this model can helps in dental diagnosing and to evaluate the orthogonal mechanical properties values especially for edentulous patients. The noises produced for filling cavity materials or dental implants are eliminated by combined classical segmentation techniques. Tetrahedral elements are suitable to divide the mandible model to finite elements for mechanical analysis studies like implant stress-strain; multi-objects technique separate mandible to objects for decreasing the number of nodes and elements to reduce the number of FEA equations; this will accelerate the idealization process at FEM models.

5. References:

- [1] Weinstein, A.M, Klawitter, J.J, Anand, S.C, and R. Schuessler, "Stress Analysis of Porous Rooted Dental Implants" *J Dent Res, Volume 55(5)*, pp. 772-777, 1976.
- [2] Atmaram, G.H, Mohammed, H., and F.J. Schoen," Stress analysis of single-tooth implants. I. Effect of elastic parameters and geometry of implant" *Artificial Cells, Blood Substitutes and Biotechnology*, Conf, *Volume 7(1)*, pp. 99-104, 1979.
- [3] Atmaram, G.H., and H. Mohammed, "Stress Analysis of Single-Tooth Implants II. Effect of Implant Root-Length Variation and Pseudo Periodontal Ligament Incorporation" *Artificial Cells, Blood Substitutes and Biotechnology, Volume 7(1)*, pp.105-110, 1979.
- [4] Mohammed, H., Atmaram, G.H., and F.J. Schoen, "Dental implant design: a critical review" *J Oral Implantol, Volume 8(3)*, pp. 393-410, 1979.
- [5] Borchers, L., and P. Reichart," Three-dimensional stress distribution around a dental implant at different stages of interface development" *J Dent Res, Volume 62(2)*, pp. 155-159, 1983.
- [6] Cook, S.D., Weinstein, A.M., J.J. Klawitter," A three-dimensional finite element analysis of a porous rooted Co-Cr-Mo alloy dental implant" *J Dent Res, Volume 61(1)*, pp. 25-29, 1982.
- [7] Meroueh, K.A., Watanabe, F., and P.J. Mentag, "Finite element analysis of partially edentulous mandible rehabilitated with an osseointegrated cylindrical implant" *J Oral Implantol, Volume 13(2)*, pp. 215-238, 1987.
- [8] Williams, K.R., Watson, C.J., Murphy, W.M., Scott, J., Gregory, M., and D. Sinobad," Finite element analysis of fixed prostheses attached to osseointegrated implants" *Quintessence Int, Volume 21(7)*, pp. 563-570, 1990.
- [9] Akpinar, I., Demirel, F., Parnas, L., and S. Sahin," A comparison of stress and strain distribution characteristics of two different rigid implant designs for distal extension fixed prostheses" *Quintessence Int, Volume 27(1)*, pp. 11-17, 1996.
- [10] Shum, H.Y., Chan, S.C. and S.B. Kang, *Image-Based Rendering*, Springer Science-Business Media, LLC, Spring Street, New York, USA, 2007.
- [11] Ruijven, van. L.J., Mulder, L., and T.M.G.J. van Eijden, "Variations in mineralization affect the stress and strain distributions in cortical and trabecular bone", *J. Biomech. Eng., Volume 40(6)*, pp. 1211-1218, 2006.
- [12] Tognola, G., Parazzini, M., Pedretti, G., Ravazzani, P., Grandori, F., Pesatori, A., Norgia, M., and C. Svelto, "Optimization of 2D to-3D Reconstruction Technique for Maxillofacial Surgery Applications", Proceedings of IEEE/IST International Workshop on Imaging Systems and Techniques, pp.186-189, Italy, April 2006.
- [13] Tognola, G., Parazzini, M., Pedretti, G., Ravazzani, P., and C. Svelto," Three-dimensional reconstruction and image processing in mandibular distraction planning" *IEEE transaction on instrumentation and measurement, Volume. 55(6)*, pp.1959-1964, December 2006.
- [14] Tognola, G., Parazzini, M., Pedretti, G., Ravazzani, P., Grandori, F., Pesatori, A., Norgia, M., and C. Svelto, "Novel 3D reconstruction method for mandibular distraction planning" Proceedings of the 2006 IEEE International Workshop on [Imaging read Imaging], pp.82-85, Italy, April 2006.
- [15] Pileicikiene, G., Varpotas, E., Surna, R., and A. Surna," A three-dimensional model of the human masticatory system, including the mandible, the dentition and the temporomandibular joints", *Stomatologija, Baltic Dental and Maxillofacial Journal, Volume. 9 (1)*, pp.27-32, 2007.
- [16] M. Chen , L. Ni , Yu Zhang , Yuan Zhang " Comparison study on the 3D reconstruction of mandible according to Virtul Chinese Human slice data and CT data", *World Journal of Modelling and Simulation, Volume. 3 (3)*, pp. 235-240, May 2007.
- [17] Liu, Z., Fan, Y., and Y. Qian, " Biomechanical simulation of the interaction in the temporomandibular joint within dentate mandible: a finite element analysis", Proceedings of IEEE/ICME International Conference on Complex Medical Engineering, pp.1842-1846, Beijing, 2007.
- [18] Reina, J.M., García-Aznar, J.M., Domínguez, J., and M. Doblaré, "Numerical estimation of bone density and elastic constants distribution in a human mandible", *J. Biomech. Eng., Volume 40 (6)*, pp. 828-836, March 2006.
- [19] Langdon, J.D., Berkovitz, B.K.B and B.J. Moxham, *Surgical Anatomy of the Infratemporal Fossa*, Special ed., Martin Dunitz, Taylor & Francis Group plc, London, New Fetter Lane, 2005.
- [20] Campadelli, P., Casiraghi, E., Pratissoli, S., and G. Lombardi," Automatic abdominal organ segmentation from CT images", *Electronic Letters on Computer Vision and Image Analysis, Volume 8(1)*, pp.1-14, January 2009.